2011

# Improved cellular infiltration into nanofibrous electrospun crosslinked gelatin scaffolds templated with micrometer sized polyethylene glycol fibers

Maciej Skotak
*University of Nebraska-Lincoln*, m.skotak@gmail.com

Jorge Ragusa
*University of Nebraska-Lincoln*, jorgeragusa@gmail.com

Daniela Gonzalez
*University of Nebraska-Lincoln*

Anuradha Subramanian
*University of Nebraska-Lincoln*, asubramanian2@unl.edu

Published in final edited form as:
*Biomed Mater*. 2011 October ; 6(5): 055012. doi:10.1088/1748-6041/6/5/055012.


# Improved cellular infiltration into nanofibrous electrospun cross-linked gelatin scaffolds templated with micrometer sized polyethylene glycol fibers

**Maciej Skotak**[1], **Jorge Ragusa**[2], **Daniela Gonzalez**[2], and **Anuradha Subramanian**[2,*]

[1]Biomechanics, Biomaterials and Biomedicine Instrumentation Facility, College of Engineering, University of Nebraska-Lincoln, NE 68588-0642

[2]Department of Chemical and Biomolecular Engineering, University of Nebraska-Lincoln, NE 68588-0643

## Abstract

Gelatin-based nanofibrous scaffolds with a mean fiber diameter of 300 nm were prepared with and without micrometer-sized polyethylene glycol (PEG) fibers that served as sacrificial templates. Upon fabrication of the scaffolds via electrospinning, the gelatin fibers were crosslinked with glutaraldehyde, and the PEG templates were removed using *tert*-butanol to yield nanofibrous scaffolds with pore diameters ranging from 10 to 100 μm, as estimated with mercury intrusion porosimetry. Non-templated gelatin-based nanofibrous matrices had an average pore size of 1 μm. Fibroblasts were seeded onto both types of the gelatin-based nanfibrous surfaces and cultured for 14 days. For comparative purposes, chitosan-based and polyurethane (PU)-based macroporous scaffolds with pore sizes of 100 μm and 170 μm, respectively, also were included. The number of cells as a function of the depth into the scaffold was judged and quantitatively assessed using nuclei staining. Cell penetration up to a depth of 250 μm and 90 μm was noted in gelatin scaffolds prepared with sacrificial templates and gelatin-only nanofibrous scaffolds. Noticeably, scaffold preparation protocol presented here allowed the structural integrity to be maintained even with high template content (95 %) and can be easily extended towards other classes of electrospun polymer matrices for tissue engineering.

## 1 Introduction

In the context of tissue engineering, the effect of micro-topography as afforded by scaffold morphology is an important design parameter, as porosity, pore size, and pore-interconnectivity are all factors that impact cellular infiltration and colonization of scaffolds. Over the last five to ten years, there has been an interest in the fabrication of scaffolds that bear topographical and morphological similarity to the native tissues and extracellular matrix. While other established methods like melt spinning can be used to produce fibers with diameters ranging from 13 to 100 μm, the technique of electrospinning (ES) has been extensively employed to generate scaffolds with fiber diameters ranging from 100 nm to 3 μm, thus providing increased surface area per unit volume[1]. A judicious manipulation of the ES parameters such as voltage, solution viscosity, and tip-to-electrode distance allows precise control over a range of fiber diameters; however, the average pore size obtained is less than 1 μm and is a function of the random placement of the parent fibers [2]. There are abundant examples in the literature on the ability of nanofibrous scaffolds to support cell growth and proliferation; in particular, the fiber diameter and fiber orientation were found to

*To whom correspondence should be addressed: asubramanian2@unl.edu.

influence cell growth and activity [3–5]. Multiple studies have noted the lack of penetration of the cells into the nanofibrous scaffolds, since, in most cases, the pore size is much smaller than the actual cell size (~5 to 20 μm). Interestingly, elegant modeling studies have shown the mean pore radius to be a function of the fiber diameter [2] and that when fiber diameter is around 100 nm, the average pore size obtained is on the order of 10 nm at a relative density of 80%. To achieve uniform cell colonization and cellular in-growth required from many tissue-engineered equivalents, penetration into the thickness of the scaffold over the culture duration is desired. Larger pore sizes also are desired to overcome diffusional limitations in the mass transfer of nutrients [6]; however, nutrients and metabolic wastes can diffuse through the nanoporosity afforded by the electrospun mats. For example, homogenous cell distribution was reported on as-spun polycaprolactone (PCL) fibrous scaffolds (fiber OD: 4–10 μm) with pore sizes of 20–45 μm [7].

In an attempt to gain control over the pore size in nanofibrous scaffolds, recent studies have focused on engineering the porosity by using co-electrospinning methods that employ a sacrificial polymer, salt leaching, layering mats of varying fiber diameter, combining techniques of electrospinning and electrospray, and cryogenic electrospinning [8–14]. While most methods offer pore-size improvement over the scaffolds prepared from a single polymer system, the technique of co-electrospinning has attracted increased attention. Accordingly, dual-polymer composite scaffolds were prepared by co-electrospinning polycaprolactone (PCL) and polyethylene oxide (PEO, the sacrificial water soluble polymer) from two separate spinnerets, where the percent composition of PEO was varied to obtain mats with varying porosities [15]. As expected in the electrospun PCL (single component) scaffolds, cells were noted mainly on the surface, while in scaffolds containing >50% sacrificial PEO content, cells were present throughout. Interestingly, the size of PCL and PEO fibers were similar, around 1–3 μm. Unlike recently outlined methods that combine electrospinning with photopatterning to create multiscale porous scaffolds, routine electrospinning offers little spatial control over fiber deposition and fiber placement on the electrode [16]. As succinctly elucidated elsewhere, the packing density of fibers inversely correlates to the fiber diameter, which then impacts the pore size and effective mean space between the adjacent fibers [2]. Thus it appears that engineering porosity in nanofibrous mats (NFM) with fiber diameters of 100 to 300 nm is challenging when compared to mats with micrometer-sized fibers [17, 18].

Our laboratory is interested in better understanding the biosynthetic activity of articular chondrocytes on electrospun matrices, because a cell-carrier substrate that mimics the naturally occurring environment in the articular cartilage matrix is hypothesized to enable a favorable cellular response. Chondrocytes, the cell types that populate the articular cartilage, are embedded in a hierarchical matrix composed of type II collagen fibrils that range from 100 nm to 300 nm. In our previous research we have generated gelatin-based nanofibrous matrices with a mean fiber diameter of 300 nm, and this fiber diameter is roughly in the upper end of collagen fiber diameters found in articular cartilage. Similar to other studies that evaluated cellular colonization over nanofibrous matrices, our results also confirmed a lack of penetration into the depth of the scaffold; also, with increase in culture time, a dense layer of cells was noted on the nanofibrous surface, and a modest penetration of 30 μm was noted over a 1 mm scaffold [19].

Thus, in this study, we were motivated to incorporate porosity and to attain higher pore sizes to facilitate infiltration and cellular in-growth, while keeping the fiber diameter of the parent fiber at 300 nm. We employed electrospinning to generate a composite matrix with parent gelatin fibers and polyethylene glycol (PEG) fibers, which served as the sacrificial component. In order to engineer porosity in a 300-nm NFM, the sacrificial polymer (PEG) was electrospun to yield fibers 3–6 μm in diameter. Prior to removal of PEG, gelatin

nanofibers were crosslinked with glutaraldehyde to confer structural integrity. The pore size distribution in nanofibrous mats prepared from pure gelatin and a gelatin-PEG system was assessed by mercury intrusion porosimetry. The morphology of cell-seeded scaffolds and bare scaffolds was visualized by scanning electron microscopy [20]. Finally, cells were seeded and maintained in culture for 14 days, and the cellular infiltration was quantitated by nuclear staining and subsequent estimation of cell numbers and depth into the scaffold. Cellular infiltration over nanofibrous scaffolds prepared in our laboratory was compared with macroporous scaffolds.

## 2 Experimental

### 2.1 Chemicals and reagents

Gelatin (powder, type B from bovine skin, approx. 225 Bloom) and 2,2,2-trifluoroethanol (TFE, >99%) were purchased from Aldrich. Polyethylene glycol (PEG, average $M_n$=8,500–11,500), polyethylene oxide (PEO, $M_v$=1,000,000), *tert*-butanol (t-BuOH, 99.5%), ether (anhydrous, 99+%) and glutaraldehyde (GA, 50% in $H_2O$, suitable for photographic applications) were purchased from Sigma-Aldrich. Anhydrous ethanol (EtOH, >99.5%) was purchased from McCormick Distilling Co., Inc. (Weston, MO), and glacial acetic acid (99.7%, AcOH) was purchased from EM Science (Gibbstown, NJ). Polyurethane-based open cell scaffold was received as a generous gift from Biomerix, Inc. (Freemont, CA). The patented polymeric scaffold is a flexible, biodurable, crosslinked, reticulated elastomeric polycarbonate-polyurethane-urea based 3-D scaffold matrix with > 95% voids and with interconnected and inter-communicating network of fully accessible pores. Chitosan (degree of deacetylation of 80%) was purchased from Vanson Halosource, Inc. (Redmond, WA). All chemicals and materials were used as received.

### 2.2 Scaffold preparation

**2.2.1 Freeze-dried chitosan (FDC)—**These scaffolds were prepared by the freeze-drying method detailed elsewhere [21]. Briefly, 2 mL of a 2% (w/v) solution of chitosan in 1% acetic acid were pipetted into each well of a 24-well tissue culture polystyrene plate (TCP, Falcon brand, Fisher, PA). The samples were frozen at −20 °C and lyophilized for 24 to 36 hours. The scaffolds were then cut with a biopsy punch into specimens of 5 mm OD and 5 mm thickness. Subsequently, scaffolds were neutralized with 0.25 M NaOH for 30 min., and rinsed with deionized water (DI) three times. Sterilization was performed with 70% ethanol solution (1 hour), followed by rinsing with sterile DI, and scaffolds were incubated overnight in DMEM-F12 medium with 10% fetal bovine serum (FBS).

**2.2.2 Non-templated gelatin nanofibrous (GNF) scaffolds—**Electrospinning of gelatin was performed from freshly prepared solutions of 10% (w/v) gelatin in 10% (v/v) AcOH/TFE solutions as described elsewhere [19] to obtain gelatin fibers with a mean diameter of 300 nm. The flow rate (0.2 mL/h) was controlled using a precise syringe pump (Cole-Parmer 74900-00, Vernon Hills, IL). Working distance (nozzle tip to collector) was 10 cm, and the applied voltage was 5 kV (Gamma High Voltage Research ES30 P-1575W/PRG, Ormond Beach, FL). Glutaraldehyde cross-linked, [19] non-templated GNF scaffolds were used as a negative control in cell infiltration studies.

**2.2.3 Templated gelatin nanofibrous (TGNF) scaffolds—**Preliminary electrospinning experiments with PEG solutions were carried out to establish a set of processing parameters in order to obtain micrometer-sized PEG fibers. Polymer solutions with concentrations ranging from 25% to 60% w/v were used in separate experiments; theconcentration of PEO was kept constant at 1% w/v. Addition of PEO was made to render PEG solutions spinnable. The following solvent systems were tested: TFE, EtOH-$H_2O$ (3:1)

and EtOH-$H_2O$-ether (2:1:1). The addition of highly volatile solvent (ether) proved to increase the fiber diameter in a previous study [22], but mats produced using EtOH-$H_2O$-ether (2:1:1) solvent system were highly delaminated. Furthermore, PEG/PEO fibers produced using TFE as a solvent were polydisperse. Thus, EtOH-$H_2O$ (3:1) was used in all experiments to generate PEG fibers.

All electrospinning experiments were performed using three Hamilton syringes (5 or 10 mL) equally spaced (120°) on the perimeter of the rotating mandrel setup and pointing inward toward the collector located in the center (Figure 1). Flow rates of 0.5 and 1.0 mL/h were used to vary gelatin-to-PEG ratio in the prepared constructs. The fibers were deposited onto Al foil tightly wrapped around the collector (a mandrel with 5 cm OD and 7.5 cm height) rotating at 60 rpm.

Gelatin nanofibrous scaffolds with PEG supported on aluminum foil were excised from the collected mat (1.5 cm × 7 cm, 1 mm thickness). Two specimens thus prepared were placed in a Petri dish and immersed in 10 mL of a 1% GA in t-BuOH solution. Vessels were covered with a watch glass and cross-linking was carried out for 1 hour at 30 °C. Samples then were removed from the cross-linking solution, washed and transferred to 30 mL vials filled with pure t-BuOH. The vials were set for 24 hours in a water bath kept at 60 °C to remove the PEG template. The hot solution of the polymer in t-BuOH was removed immediately and TGNF samples were frozen (−21 °C), lyophilized overnight, and stored in zip-lock bags until further use.

### 2.3 Cell seeding

Samples were sterilized by contact with 70% ethanol for one hour. Sterilized samples were washed with sterile PBS, rinsed with deionized water, and then wetted in RPMI medium for 2hours prior to cell seeding. Two (GNF/TGNF: 10 × 10 mm) or three (FDC/polyurethane [PU]: OD 5 mm) specimens were placed on the bottom of the wells of a 6-well polystyrene tissue culture plate (TCP; Falcon brand, Fisher, PA). A total of 24 scaffolds per secimen were used. The fibroblasts (cell line L929; ATCC) were seeded onto the pre-wetted scaffolds and maintained for 3 hours in the incubator at 37 °C. Cell seeding density was a) PU/FDC: $3 \times 10^4$, and b) GNF/TGNF: $1.5 \times 10^5$ cells per scaffold. Subsequently, 8 mL of medium were added to each well. Cells were cultured in DMEM-F12 medium (Gibco, NY) plus 10% fetal bovine serum and 1× antibiotic-antimycotic (Gibco, NY). The 6-well TCP was kept in a cell culture incubator at 37 °C, 95% humidity and 5% $CO_2$, and the medium was changed every 3 days. After 14 days the samples were fixed and analyzed by SEM, confocal microscopy, and assays.

### 2.4 Whole mount stain

Upon the completion of the cell culture step and fixation with 4% formaldehyde (Electron Microscopy Sciences, Hatfield, PA) for 12 hours at room temperature, scaffolds seeded with cells were washed with 1× PBS and permeated with 0.1% Triton X-100 (for molecular biology, Sigma) in 1× tris buffered saline (TBS), washed in TBS, blocked with 1% bovine serum albumin (OmniPur, fraction V, lot# 1726B003) in TBS, then incubated with 1:1 mixture of Sytox® Green (Invitrogen, diluted 1:5000) and Alexa Fluor® 594 phalloidin conjugate (Invitrogen, diluted 1:50) solution for 30 minutes at room temperature.

### 2.5 Characterization

**2.5.1 Cell count and cytoskeletal visualization—**After completion of cell culture, Sytox® Green DNA stain was used to mark fibroblast nuclei on scaffolds. In order to determine cell quantity through scaffold profundity, images of stained nuclei at different depth levels were acquired using confocal microscopy (Olympus IX 81). Two or three z-

stack images with a step size of 10 μm were taken arbitrarily from 5 PU, 5 FDC, 15 GNF, and 21 TGNF samples. Cell counting was performed using ImageJ 1.43u software. The F-actin fibrils were visualized with phalloidin – Alexa Fluor® 594 conjugate using confocal microscopy. All images were collected with 20× magnification objective and were sequenced at a constant step size of 1 μm (z-section).

**2.5.2 Cell viability and proliferation using MTS assay—**Cell viability was assessed by MTS/PMS colorimetric assay (3-[4,5-dimethylthiazol-2-yl]-5-[3-carboxymethoxyphenyl]-2-[4-sulfophenyl]-2H-tetrazolium and phenazine methosulfate, respectively). A total of 3 samples per specimen were tested using a 12-well TCP plate (a single scaffold per well). The cell culture media were removed and 1 mL of PBS was transferred to each well. Then 200 μL aliquots of the MTS/PMS solution were pipetted into each well, and the plate was put inside the cell culture incubator (37 °C, 5% $CO_2$ atmosphere) for 4 hours. The 250 μL aliquots of the supernatant were transferred to four wells of a new 96-well plate, and the absorbance at 490 nm was measured using the Elx800™ universal microplate reader (BioTek Instruments, Inc., Winooski, VT).

**2.5.3 SEM imaging—**Non-coated samples of gelatin nanofibers and PEG microfibers from GNF and TGNF specimens were analyzed on a Quanta 200 FEG Environmental SEM using an accelerating voltage in the range of 8–10 kV and a 6000 magnification. Statistical analysis of PEG template fibers was performed on sets of at least three different SEM images, which corresponds to at least 50 counts within each specimen.

Scaffolds seeded with fibroblasts were first taken out of the cell culture medium, rinsed with and inundated in phosphate buffered saline (PBS) for 15 minutes. The same step was repeated one more time, and after PBS removal, enough volume of 2.5% GA/PBS solution to cover the samples was added. Fixation with GA was performed for 30 minutes, followed by its removal and subsequent rinsing with PBS. After discarding the PBS supernatant, the samples were dehydrated with ethanol gradient (40, 50, 70, 95, and 100%), and critical point drying (CPD) was performed. The SEM images were collected according to the protocol described elsewhere [23]. Briefly, before SEM characterization samples were coated with metallic gold for 2 minutes, while the electrical current inside the chamber of the Technics Hummer II sputter coater remained constant (10 mA). Hitachi S-3000N microscope was set to high vacuum mode and an accelerating voltage of 25 kV was used.

**2.5.4 Differential scanning calorimetry (DSC)—**Studies were realized using a Q100 machine (TA Instruments, New Castle, DE). An empty hermetic Al pan was used as a reference. The DSC was calibrated for temperature (melting point 156.6 °C) and heat flow ($\Delta H_m$, 28.45 J/g) using indium. Typically, a 6–8 mg sample was sealed in the hermetic aluminum pan, then placed in the sample compartment, equilibrated at 0 °C, and heated to a final temperature of 160 °C. A heating rate of 10 °C/min. was used, and the sample compartment was flushed with dry nitrogen flowing at a rate of 25 mL/min.

**2.5.5 Mercury intrusion porosimetry—**Mercury intrusion porosimetry (MIP) technique was selected to evaluate the pore size diameters (PSD) for selected samples. Measurements were performed in the Particle Engineering Research Center at the University of Florida. Quantachrome Autoscan 60 Mercury Porosimeter was used to analyze the samples, and Quantachrome Autoscan Poro2PC (Version 3.0) software was used to generate pore-related data.

# 3 Results and discussion

## 3.1 Electrospinning of PEG template microfibers

In this study we sought to incorporate PEG fibers with parent gelatin fibers to serve as sacrificial templates in an attempt to enhance matrix porosity. We further hypothesized that PEG fibers with diameters at least 10-times greater than the parent gelatin fibers are desirable in increasing the porosity of TGNF scaffolds. Both GNF and TGNF were produced using the setup [8] schematically depicted in Figure 1. In this study, we aimed to prepare gelatin fibers with mean diameters of 300 nm, which are roughly in the upper end of collagen fiber diameters found in articular cartilage. We have previously reported on the preparation and characterization of 300 nm gelatin fibers [19]. Briefly, in order to produce GNF with a mean diameter of 300 nm, a flow rate of 0.2 mL/h, a voltage of 5 kV, and a needle-collector distance of 10 cm were employed. As schematically shown in Figure 1A, TGNF scaffolds were fabricated using two syringes with gelatin and one with PEG, equally spaced (120°) around the perimeter of a rotating mandrel collector. The same setup was used for the fabrication of GNF scaffolds, where all three syringes supplied gelatin solution.

Hence, we have undertaken a study to optimize the electrospinning process with respect to PEG, where, notably, low molecular weight polymer (MW = 10 kDa) was used to prepare sacrificial templates in our studies. The rationale behind this choice is dictated by the assumption that lower molecular weight PEG is easily dissolved when compared to high molecular weight counterparts (e.g., PEO) that are often used as templates to enhance porosity of electrospun scaffolds [8, 10, 15, 24]. Attempts to electrospin pure PEG solutions were not successful, irrespective of the solvent system used [25]. It was necessary to add up to 1% by weight of 100 kDa PEO to render PEG solutions spinnable. Thus our first objective was to prepare PEG microfibers from solutions that contained 50 wt% PEG and 1 wt% PEO. The relationship between PEG fiber diameter and experimental variables, namely, flow rate and voltage, are depicted in Figure 2. It is notable that PEG fibers with larger diameters were obtained at higher flow rates, and smaller PEG fiber diameters were produced at higher voltages. Therefore, in order to produce PEG fibers with the biggest diameter, a voltage of 5 kV was selected since it is the same voltage used for the fabrication of gelatin nanofibers. This enabled us to maintain similar tip-to-electrode distances for both gelatin and PEG. Highly concentrated polymer solutions (e.g., PEG) are known to produce fibers with higher diameters [23, 26, 27]; thus studies were undertaken to evaluate the spinnability of 60 wt% and 70 wt% PEG. The viscosity of PEG solutions at 70 wt% or higher precluded their usage; 60 wt% PEG and 1 wt% PEO were tested at two flow rates at 5 kV, and the resultant fiber diameters are shown in the inset of Figure 2. In all subsequent experiments, a solution of 60 wt% PEG and 1 wt% PEO in water-ethanol (1:3) solution was electrospun to yield fibers with a nominal diameter of 6.3 ± 1.84 micrometers.

## 3.2 Preparation of highly porous gelatin nanofibrous scaffolds

Control over porosity was achieved by varying the PEG-to-gelatin mass ratio. Constructs with ratios (PEG to gelatin) of 3, 9, 15, and 18 were fabricated and all resulting scaffold materials were evaluated for stability upon template removal, and porosity was determined via mercury intrusion analyses. Scaffold materials that yielded the highest porosity with stability were chosen for subsequent cell culture studies. It turned out scaffolds produced at all PEG-gelatin ratios were prone to delamination with lamellae thicknesses of approximately 200 μm when 50% PEG/1%PEO solutions were used. This is typically observed when electrospinning is employed to manufacture constructs with thicknesses exceeding 1 mm (see, for example, Figure 3 in [11]). Simple increase of the PEG concentration to 60% was a remedy for this problem, and scaffolds with improved structural integrity were produced. We relate this to the increased solvent entrapment within PEG

fibers. Hence, incompletely dried template fibers act as “glue” and helped to preserve structural integrity of scaffolds.

The removal of PEG sacrificial fibers was performed in the hot t-BuOH. It is worth to note ethanol, frequently used as a co-solvent for electrospinning of high molecular weight PEO is a non-solvent for either PEG or PEO at room temperature. During early stage of the project on gelatin nanofibrous scaffolds we have attempted to use 1-propanol as a solvent for glutaraldehyde to facilitate cross-linking. These attempts were only partially successful. The gelatin was stabilized (cross-linked), but the structural integrity of non-templated gelatin scaffold was compromised due to action of capillary forces. We have observed similar phenomenon for scaffolds made of electrospun nanofibrous polyurethane/gelatin (core-shell) scaffolds: after removal of gelatin “shell” using water the scaffold porosity was lost (unpublished data from our laboratory). Water used for template removal caused the scaffold structure to collapse. Similarly, PEO template removed with water from nanofibrous poly-L-lactide (PLA) constructs caused complete collapse of the structure (unpublished data). The coalescence of the nanofibers in these scaffolds is driven by capillary forces associated with high surface tension of water ($\gamma$ = 71.79 mN/m at 25 °C), similarly to bundling of individual elastic fibers of the paintbrush [28]. As the solvent enters the pores of the material it causes coalescence of adjacent fibers and this ultimately leads to the loss of original structure and porosity. For low surface tension solvents (for example ethanol $\gamma$ = 22.27 mN/m at 20 °C) the entrance of the solvent did not cause any adverse effects in our experiments but porosity was lost upon solvent removal. The simple remedy to prevent the destructive action of capillary forces is to use low surface tension solvent followed by freeze drying to remove the residual solvent. Thus, the t-BuOH was our solvent of choice; thanks to a relatively high melting point (25 °C) it is appropriate for lyophilization and a suitable solvent for PEG solubilization at 60 °C. To the best of our knowledge, we are unaware of similar research describing t-BuOH to control and protect the porosity of scaffolds by preventing surface tension and capillary forces associated effects.

For further evaluation based on the mercury intrusion porosimetry results (not shown), the scaffolds with the highest allowable PEG-to-gelatin mass ratio of 18:1 were selected, as previous studies have shown improved cellular infiltration with increasing content of subsequently eliminated sacrificial fibers [15]. Note, on the contrary to the work of Baker and colleagues, who reported scaffolds’ collapse when 80 % or more (by mass) of the sacrificial PEO fibers were removed (figure 5, in [15]), our scaffold preparation protocol allowed to maintain the structural integrity with removed template content as high as 95 %. Immersion in the cell culture media resulted only in minimal shrinkage.

The gross morphologies of the scaffolds employed in this study were observed via SEM and are shown in Figure 3. Figures 3A and 3B show PU and FDC scaffolds, and the macroporous nature of these scaffolds is readily evident. GNF scaffolds, composed of only 300-nm gelatin fibers, are shown in Figure 3C. TGNF scaffolds, composed of parent gelatin fibers (300 nm) and sacrificial PEG templates (~6 μm), are shown in Figure 3D, where the PEG microfibers embedded onto gelatin matrix can be clearly seen. PEG sacrificial microfibers exceed gelatin nanofiber diameter by a factor of 20. PEG fibers were leached out using t-BuOH, and the resultant scaffold material is shown Figure 3E, clearly illustrating the absence of sacrificial PEG microfibers. The presence of micrometer size pores in TGNF scaffolds with PEG removed can be noted in Figure 3E, a feature that is not observed in the packed GNF structure in Figure 3C.

Due to the hydrophilic nature of both polymers used in this study (gelatin and PEG), and in spite of the fact that the former was stabilized by cross-linking with GA, we did not used water to remove the template (as discussed earlier). At room temperature the t-BuOH is a

non-solvent for both polymers, but when the temperature is increased to 60 °C, PEG dissolves in t-BuOH. Thus, the structure of the gelatin nanofibrous scaffold was not compromised, and the template fibers were dissolved in hot t-BuOH in merely 24 hours (without mixing). This is considerably shorter than the typical time required for dissolution of high molecular weight PEO (100 kDa, 7 days) [24]. The efficacy of the PEG removal via extraction with t-BuOH was evaluated with DSC (Figure 4). A long inverted peak at a minimum of 65 °C, the melting point of PEG, can be seen in the DSC profile of pure PEG (scan D). A similar peak at 65 °C also can be noted for TGNF scaffolds with embedded PEG microfibers (scan C). However, in samples of TGNF scaffolds with sacrificial PEG microfibers removed (scan B), a very small peak was noted at 55 °C. Judging by the peak area, a 90% removal of the PEG microfiber templates can be estimated by washing with two 30 mL t-BuOH aliquots. Complete removal of the PEG fibers may require harsher conditions than were employed in this study.

The pore size distributions (PSD) in the various scaffolds included in this study were ascertained by mercury intrusion porosimetry [24] and are shown in Figure 5. The PSDs of FDC and PU scaffolds were observed to be unimodal, with mean pore size values of 100 and 170 μm, respectively, and were confirmed by SEM images. On the contrary, GNF and template-removed TGNF scaffolds present bimodal distributions. Pore sizes of 1 μm are predominant for GNF, with few pores in the 10–100 micrometer range. Although a similar peak is evident in template-removed TGNF, an increment in the density and distribution of large pores is distinguishable (Figure 5).

### 3.3 Cellular infiltration and morphology

Cells were seeded on the matrices and maintained in culture for 14 days. The differences in the initial seeding density were to account for the available surface area of the scaffolds, compensate for different geometries and to provide similar initial cell densities. PU and CHIT scaffolds are round (OD = 5 mm), while GNF/TGNF scaffolds are squares (side length = 10 mm) with top surface area 20 $mm^2$ and 100 $mm^2$, respectively. Hence five times more cells were seeded on gelatin based scaffolds to attain similar initial cell densities (cells per unit surface area) as that of PU/CHIT scaffolds. Relatively high viabilities for all samples were estimated by MTS assay (Figure 6). In particular, the cellular viabilities on GNF and template-removed TGNF scaffolds were similar. The gross cellular morphologies on PU, FDC, GNF, and TGNF scaffolds are shown in Figure 7. As reported by our group and others [19], cells (~10 μm in diameter) populated exclusively only the top surface on GNF scaffolds (Figure 7C), whereas on TGNF scaffolds with template removed, cells are embedded in the gelatin fibrous matrix (Figure 7D). In this study, we have used confocal imaging, optical sectioning, and image processing to compute the number of cells as a function of scaffold depth. The results of the analysis are shown in Figure 8. Cell counts are presented in logarithmic scale for each specimen as a function of scaffold depth, with the top layer of the scaffold representing zero level. At the end of 14 days, on both PU and highly porous FDC scaffolds, cellular infiltration up to a scaffold depth of 600 μm and 300 μm, respectively, was observed. While both FDC and PU scaffolds are macroporous, PU scaffolds possess an open architecture that resembles a honeycomb-like structure with higher pore connectivity and 95% void content. As a result, better cellular infiltration was noted on PU scaffolds when compared to FDC counterparts. We observed cellular infiltration up to a depth of 90 μm on GNF scaffolds, corresponding to approximately five cell lengths. In contrast, on template-removed TGNF scaffolds, we detected cellular ingrowth up to 250 μm. It is worth pointing out two characteristic features of infiltration curves pertinent to scaffold porosity. The “location” of peak maximum (the scaffold depth with the highest cell count) on the cellular infiltration curves (Figure 8) is a function of the porosity of the scaffolds and decreases in the order: PU (120 μm) > FDC (100 μm) > TGNF

(60 μm) > GNF (30 μm). Simultaneously with increasing porosity of the scaffolds, the average cell count at the maximum of the infiltration curves increases in the order: PU (1080±250) < FDC (1480±540) < TGNF (3120±1730) < GNF (3460±1450). A 33% higher number of cells (~13600, an average of total cell numbers) were noted on TGNF when compared to GNF (~10200). Our data and analyses presented here suggest that the decisive parameter for cellular infiltration is pore size, not the scaffold thickness. For example, over the culture period evaluated in this paper (i.e. 14 days) the maximum infiltration of 600 μm was attained with PU scaffold which had a thickness of 5 mm.

Figure 9 shows the phalloidin-stained cytoskeleton (red) and Sytox® Green-stained nucleus (green) for the cells on the various scaffolds evaluated in this study. The F-actin staining was performed to evaluate the morphological features of fibroblasts seeded on four different types of scaffolds. It is clear from Figure 7 that a substantial number of cells attached to FDC and GNF materials have an elongated, spindle-like morphology typical of cells cultured on surfaces promoting cell spreading [4, 7, 29, 30]. Fibroblasts cultured on TGNF and PU scaffolds have a predominantly rounded shape. These findings were corroborated by F-actin staining (Figure 9). The PU is the most hydrophobic among the tested materials; hence, the round morphology of cells is not surprising [31]. However, the same is not true for TGNF scaffolds; the scaffold porosity and morphology not only facilitate cellular infiltration, they also modulate morphological features of the cells. Round morphology of fibroblasts cultured on highly porous scaffolds was reported by other groups [24]. This is an interesting outcome of the research reported here in view of future studies involving chondrocytes. These studies will include the seeding of chondrocytes on matrices with enhanced porosity and subsequent culture for 28 days. Viscoelastic properties of the resultant tissue construct will be estimated along with the expression of chondrocytic markers.

## 4 Conclusions

We have developed a facile method for the fabrication of porous cross-linked nanofibrous gelatin scaffolds and templated gelatin nanofibrous (TGNF) scaffolds. The microfibers of low molecular weight PEG which served as sacrificial templates were efficiently removed using hot t-BuOH in a relatively short time, owing to the higher vapor pressure of t-BuOH when compared to water (t-BuOH: 30.6 mmHg at 20 °C, $H_2O$: 17.5 mmHg at 20 °C). The t-BuOH appears to be an interesting solvent and, can be potentially substituted for water in applications where high surface tension of the later prevents its usage. The porosity of the TGNF scaffolds was controlled by adjusting the PEG-to-gelatin mass ratio. Improved cellular infiltration up to depths of 250 μm were noted for TGNF scaffolds, when compared to GNF and correlated with higher total cell numbers noted on TGNF. Future efforts will involve the development of methods to attain scaffold colonization throughout the depth either by using volume perfusion bioreactors [7, 24] or by further refinement of methods leading to bigger pore sizes through incorporation of template fibers with diameters exceeding 10 μm [2]. However, fiber diameters in this range are not readily prepared with a conventional electrospinning technique, and application of derivative fabrication methods, like melt electrospinning [29] or plotting [32], will be necessary.

## Acknowledgments

Partial financial support was provided by the College of Engineering and funding in-part from the National Institutes of Health (1R21RR024437-01A1). We are thankful for help received from Drs. Sanjukta Guhathakurta and Nicolas Whitney (Department of Chemical and Biomolecular Engineering, UNL). Use of electrospinning facilities in the laboratory of Dr. Gustavo Larsen (Department of Chemical and Biomolecular Engineering, UNL) is gratefully acknowledged.

## References


1. Agarwal S, Wendorff JH, Greiner A. Progress in the field of electrospinning for tissue engineering applications. Adv Mater. 2009; 21:3343–3351. [PubMed: 20882501]
2. Eichhorn SJ, Sampson WW. Statistical geometry of pores and statistics of porous nanofibrous assemblies. J R Soc Interface. 2005; 2:309–318. [PubMed: 16849188]
3. Badami AS, Kreke MR, Thompson MS, Riffle JS, Goldstein AS. Effect of fiber diameter on spreading, proliferation, and differentiation of osteoblastic cells on electrospun poly(lactic acid) substrates. Biomaterials. 2006; 27:596–606. [PubMed: 16023716]
4. Bashur CA, Dahlgren LA, Goldstein AS. Effect of fiber diameter and orientation on fibroblast morphology and proliferation on electrospun poly(D,L-lactic-co-glycolic acid) meshes. Biomaterials. 2006; 27:5681–5688. [PubMed: 16914196]
5. Nisbet DR, Forsythe JS, Shen W, Finkelstein DI, Horne MK. Review paper: a review of the cellular response on electrospun nanofibers for tissue engineering. J Biomater Appl. 2009; 24:7–29. [PubMed: 19074469]
6. Zhu XL, Cui WG, Li XH, Jin Y. Electrospun fibrous mats with high porosity as potential scaffolds for skin tissue engineering. Biomacromolecules. 2008; 9:1795–1801. [PubMed: 18578495]
7. Pham QP, Sharma U, Mikos AG. Electrospun poly(epsilon-caprolactone) microfiber and multilayer nanofiber/microfiber scaffolds: characterization of scaffolds and measurement of cellular infiltration. Biomacromolecules. 2006; 7:2796–2805. [PubMed: 17025355]
8. Baker BM, Nerurkar NL, Burdick JA, Elliott DM, Mauck RL. Fabrication and modeling of dynamic multipolymer nanofibrous scaffolds. J Biomech Eng. 2009; 131:101012-1. [PubMed: 19831482]
9. Nam J, Huang Y, Agarwal S, Lannutti J. Improved cellular infiltration in electrospun fiber via engineered porosity. Tissue Eng. 2007; 13:2249–2257. [PubMed: 17536926]
10. Ekaputra AK, Prestwich GD, Cool SM, Hutmacher DW. Combining electrospun scaffolds with electrosprayed hydrogels leads to three-dimensional cellularization of hybrid constructs. Biomacromolecules. 2008; 9:2097–2103. [PubMed: 18646822]
11. Wulkersdorfer B, Kao KK, Agopian VG, Ahn A, Dunn JC, Wu BM, et al. Bimodal Porous Scaffolds by Sequential Electrospinning of Poly(glycolic acid) with Sucrose Particles. Int J Polym Sci. 2010 2010:Article ID 436178.
12. Kidoaki S, Kwon IK, Matsuda T. Mesoscopic spatial designs of nano- and microfiber meshes for tissue-engineering matrix and scaffold based on newly devised multilayering and mixing electrospinning techniques. Biomaterials. 2005; 26:37–46. [PubMed: 15193879]
13. Leong MF, Rasheed MZ, Lim TC, Chian KS. In vitro cell infiltration and in vivo cell infiltration and vascularization in a fibrous, highly porous poly(D,L-lactide) scaffold fabricated by cryogenic electrospinning technique. J Biomed Mater Res, Part A. 2009; 91A:231–240.
14. Simonet M, Schneider OD, Neuenschwander P, Stark WJ. Ultraporous 3D Polymer Meshes by Low-Temperature Electrospinning: Use of Ice Crystals as a Removable Void Template. Polym Eng Sci. 2007; 47:2020–2026.
15. Baker BM, Gee AO, Metter RB, Nathan AS, Marklein RA, Burdick JA, et al. The potential to improve cell infiltration in composite fiber-aligned electrospun scaffolds by the selective removal of sacrificial fibers. Biomaterials. 2008; 29:2348–2358. [PubMed: 18313138]
16. Sundararaghavan HG, Metter RB, Burdick JA. Electrospun fibrous scaffolds with multiscale and photopatterned porosity. Macromol Biosci. 2010; 10:265–270. [PubMed: 20014198]
17. Balguid A, Mol A, van Marion MH, Bank RA, Bouten CV, Baaijens FP. Tailoring fiber diameter in electrospun poly(epsilon-caprolactone) scaffolds for optimal cellular infiltration in cardiovascular tissue engineering. Tissue Eng, Part A. 2009; 15:437–444. [PubMed: 18694294]
18. Gentsch R, Boysen B, Lankenau A, Borner HG. Single-Step Electrospinning of Bimodal Fiber Meshes for Ease of Cellular Infiltration. Macromol Rapid Commun. 2010; 31:59–64. [PubMed: 21590837]
19. Skotak M, Noriega S, Larsen G, Subramanian A. Electrospun cross-linked gelatin fibers with controlled diameter: the effect of matrix stiffness on proliferative and biosynthetic activity of chondrocytes cultured in vitro. J Biomed Mater Res, Part A. 2010; 95:828–836.

20. Semnani D, Ghasemi-Mobarakeh L, Morshed M, Nasr-Esfahani MH. A Novel Method for the Determination of Cell Infiltration into Nanofiber Scaffolds Using Image Analysis for Tissue Engineering Applications. J Appl Polym Sci. 2009; 111:317–322.
21. Noriega S, Mamedov T, Turner JA, Subramanian A. Intermittent applications of continuous ultrasound on the viability, proliferation, morphology, and matrix production of chondrocytes in 3D matrices. Tissue Eng. 2007; 13:611–618. [PubMed: 17518607]
22. Larsen G, Skotak M. Co-solvent mediated fiber diameter and fiber morphology control in electrospinning of sol-gel formulations. J Non-Cryst Solids. 2008; 354:5547–5554.
23. Skotak M, Leonov AP, Larsen G, Noriega S, Subramanian A. Biocompatible and biodegradable ultrafine fibrillar scaffold materials for tissue engineering by facile grafting of L-lactide onto chitosan. Biomacromolecules. 2008; 9:1902–1908. [PubMed: 18540676]
24. Lowery JL, Datta N, Rutledge GC. Effect of fiber diameter, pore size and seeding method on growth of human dermal fibroblasts in electrospun poly(epsilon-caprolactone) fibrous mats. Biomaterials. 2010; 31:491–504. [PubMed: 19822363]
25. Chen CZ, Wang L, Huang Y. Electrospinning of thermo-regulating ultrafine fibers based on polyethylene glycol/cellulose acetate composite. Polymer. 2007; 48:5202–5207.
26. Powell HM, Boyce ST. Fiber density of electrospun gelatin scaffolds regulates morphogenesis of dermal-epidermal skin substitutes. J Biomed Mater Res, Part A. 2008; 84:1078–1086.
27. Saraf A, Lozier G, Haesslein A, Kasper FK, Raphael RM, Baggett LS, et al. Fabrication of nonwoven coaxial fiber meshes by electrospinning. Tissue Eng, Part C. 2009; 15:333–344.
28. Mahadevan L, Kim HY. Capillary rise between elastic sheets. J Fluid Mech. 2006; 548:141–150.
29. Dalton PD, Klinkhammer K, Salber J, Klee D, Moller M. Direct in vitro electrospinning with polymer melts. Biomacromolecules. 2006; 7:686–690. [PubMed: 16529400]
30. Park SA, Kim IA, Lee YJ, Shin JW, Kim CR, Kim JK, et al. Biological responses of ligament fibroblasts and gene expression profiling on micropatterned silicone substrates subjected to mechanical stimuli. J Biosci Bioeng. 2006; 102:402–412. [PubMed: 17189167]
31. Harry GJ, Billingsley M, Bruinink A, Campbell IL, Classen W, Dorman DC, et al. In vitro techniques for the assessment of neurotoxicity. Environ Health Perspect. 1998; 106 Suppl 1:131–158. [PubMed: 9539010]
32. Yoon H, Kim G. A three-dimensional polycaprolactone scaffold combined with a drug delivery system consisting of electrospun nanofibers. J Pharm Sci. 2010; 100:424–430. [PubMed: 20740676]

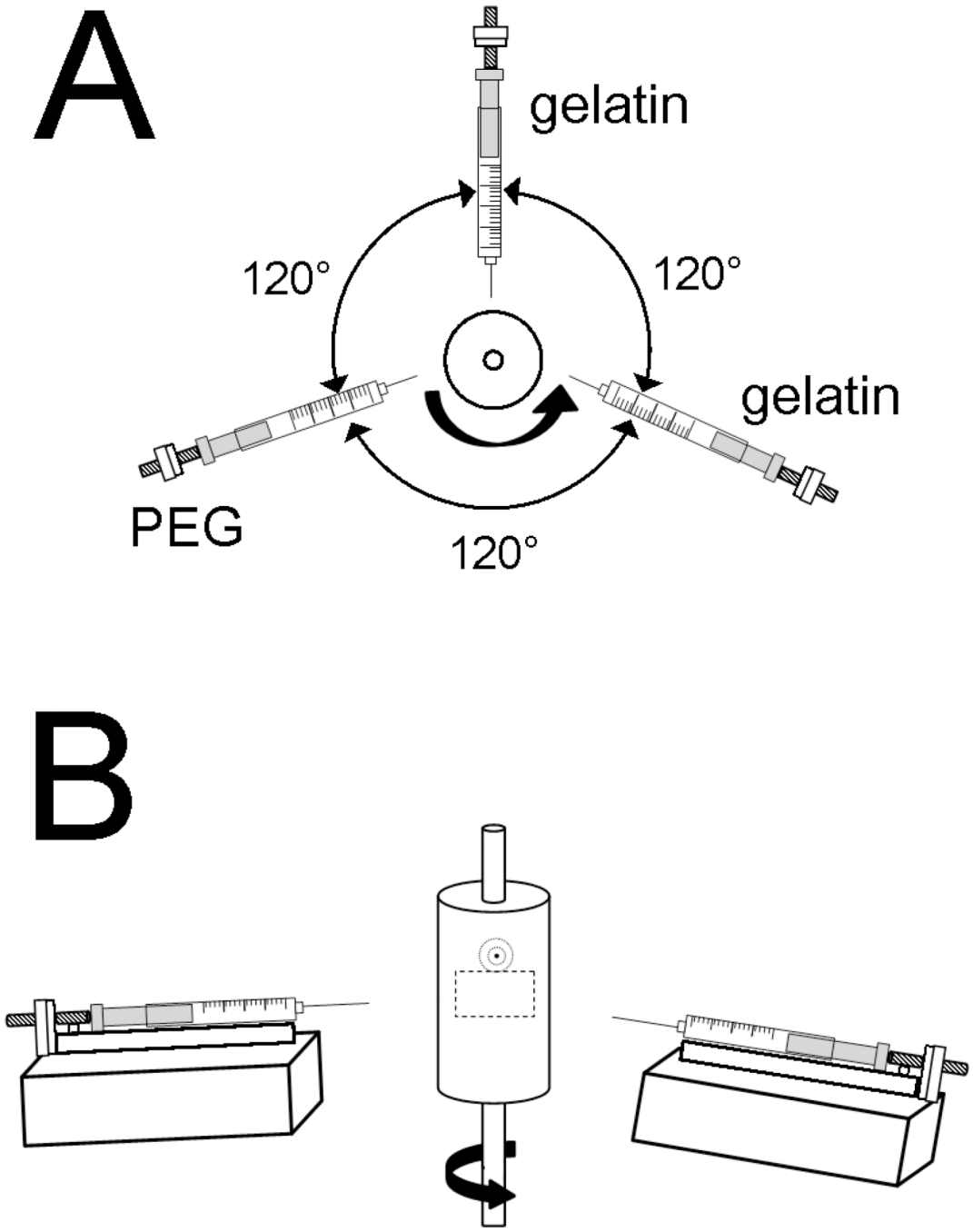


**Figure 1.**
Schematic representation of the electrospinning setup: top (A) and side view (B). Three syringes were mounted as shown and were connected to separate, individual Hamilton syringe pumps. Typically, gelatin solutions were fed via two syringes and PEG via one, and fibers were collected on the rotating mandrel.

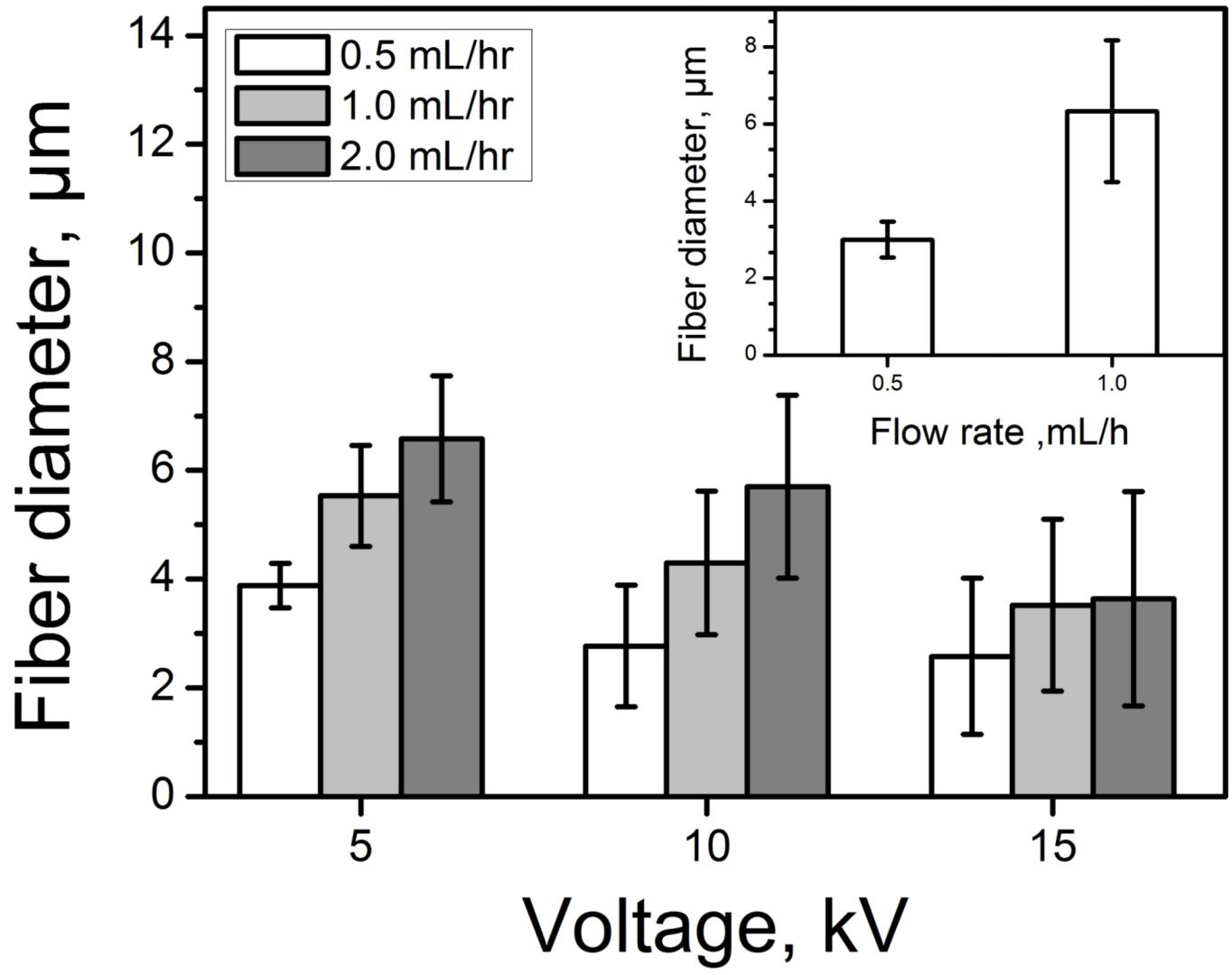


**Figure 2.**
Variation of PEG fiber diameter as a function of processing parameters. PEG microfibers fabricated using a concentration of 50% (w/v) PEG/1% PEO solution in EtOH/$H_2O$ (3:1) solvent system. Inset: the effect of the flow rate on the fiber diameter of PEG fibers prepared using 60% (w/v) PEG/1%PEO solution in EtOH/$H_2O$ (3:1). The voltage used was 5 kV and the distance needle-collector was 13 cm.

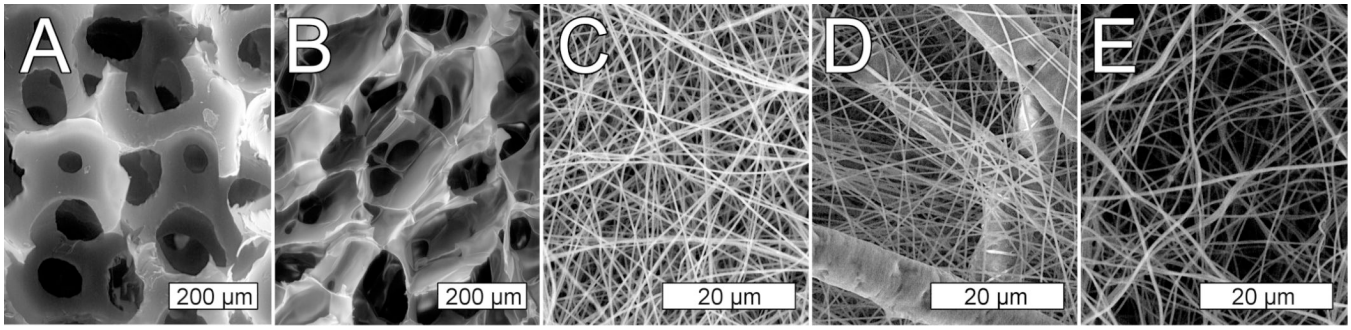


**Figure 3.**
Representative SEM images of scaffolds: A) PU, B) FDC, C) GNF (non-templated), D) TGNF with PEG microfibers embedded in the sample, E) TGNF with PEG microfibers removed.

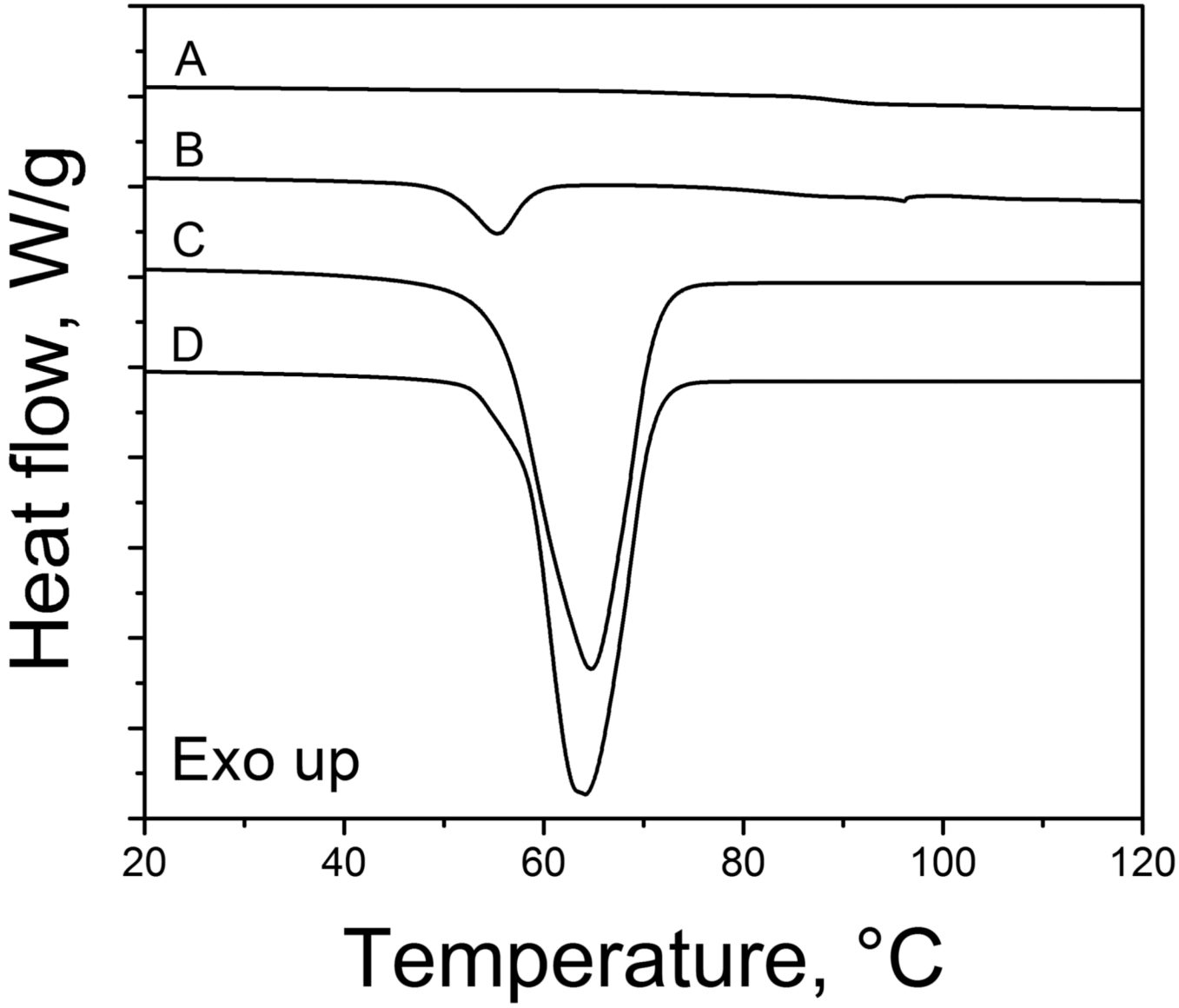


**Figure 4.**
Differential Scanning Calorimetry profiles of the scaffolds: A) GNF, B) TGNF with PEG template microfibers removed, C) TGNF with PEG template microfibers embedded in the sample, and D) bulk PEG (reference). The plots were shifted for clarity of presentation.

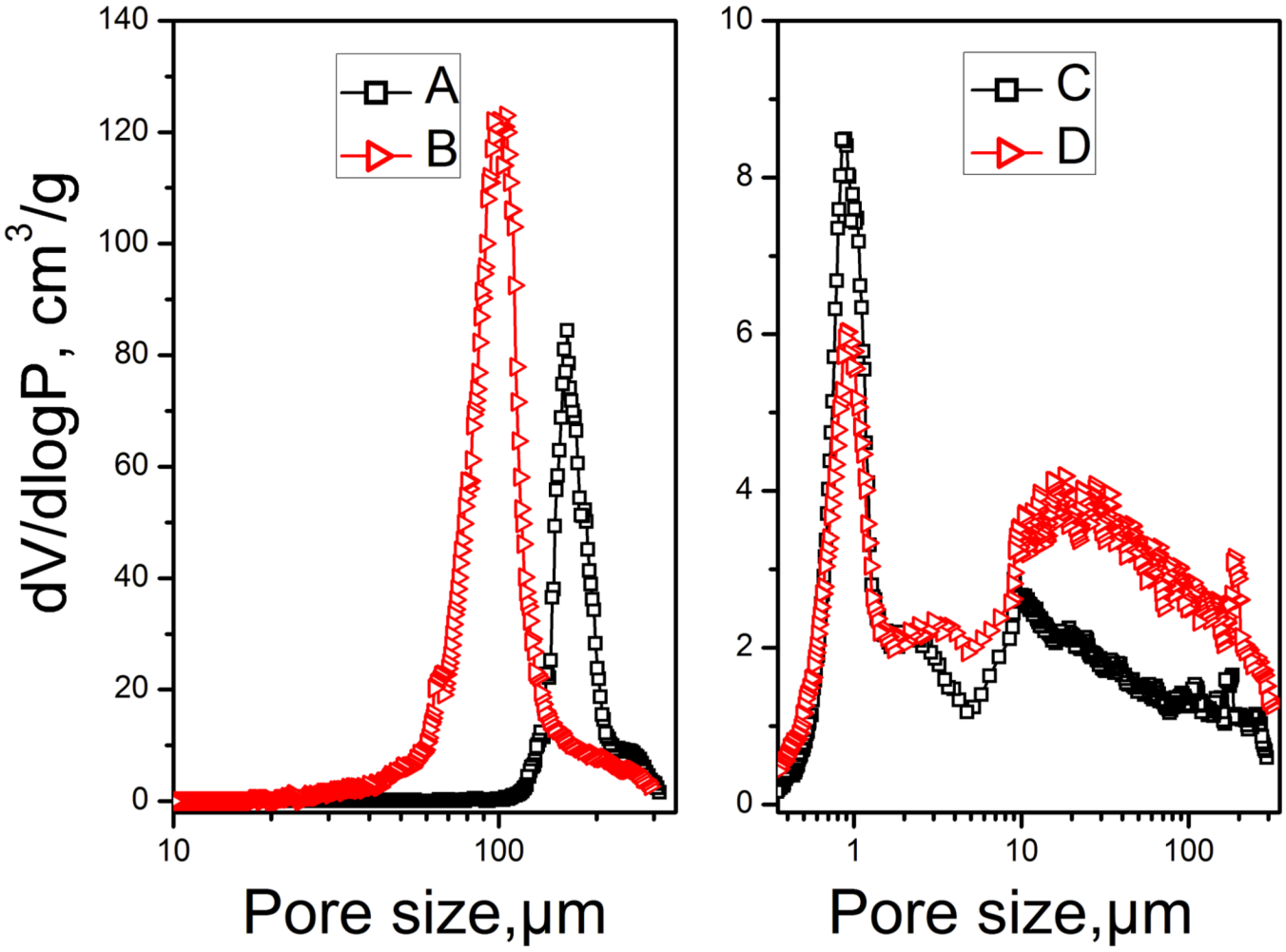


**Figure 5.**
Pore size estimations by Mercury Intrusion Porosimetry. A) PU, B) FDC, C) GNF (non-templated), D) TGNF with PEG microfibers removed (PEG-to-gelatin mass ratio 18:1).

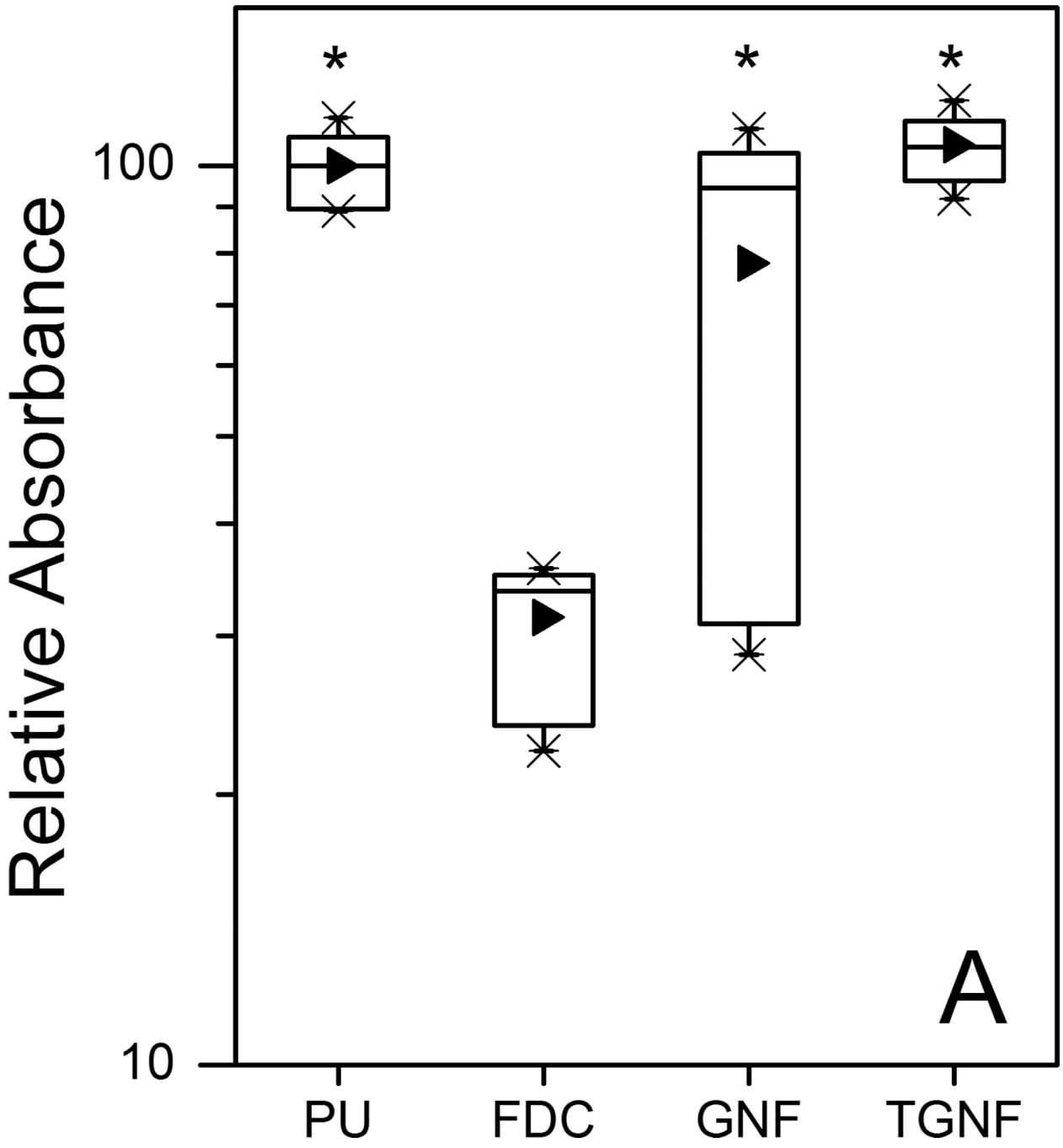


**Figure 6.**
Viability of fibroblasts evaluated by MTS assay. Normalized absorbance at 490 nm is presented.

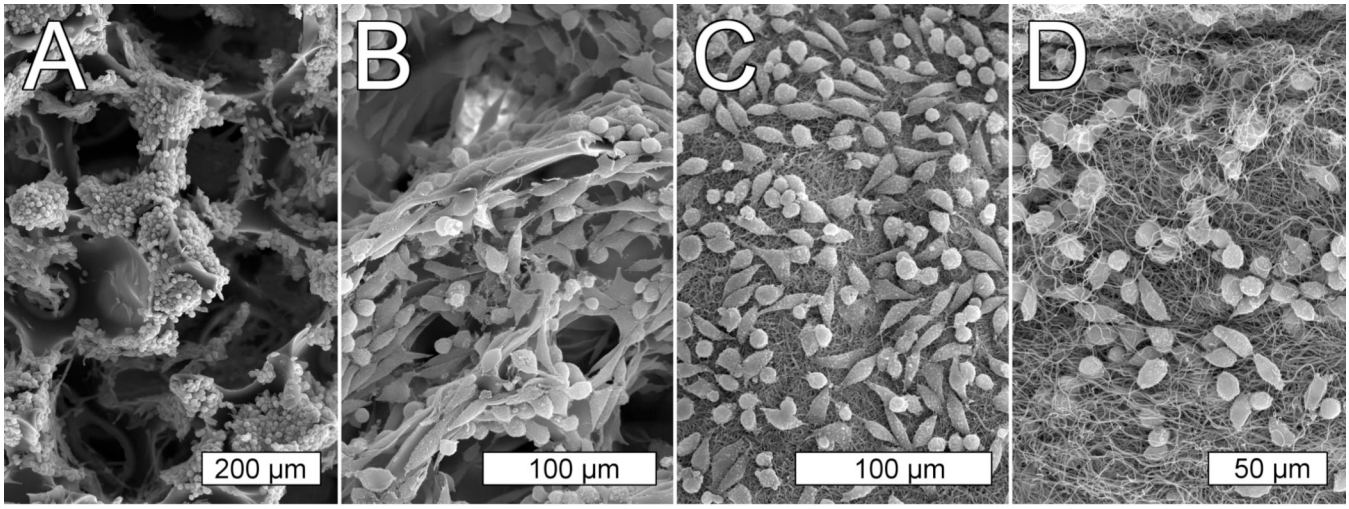


**Figure 7.**
Representative SEM images of cell-seeded nanofibrous scaffolds. Fibroblasts were seeded on scaffolds, as indicated, and maintained in culture for14 days: A) PU, B) FDC, C) GNF, and D) TGNF.

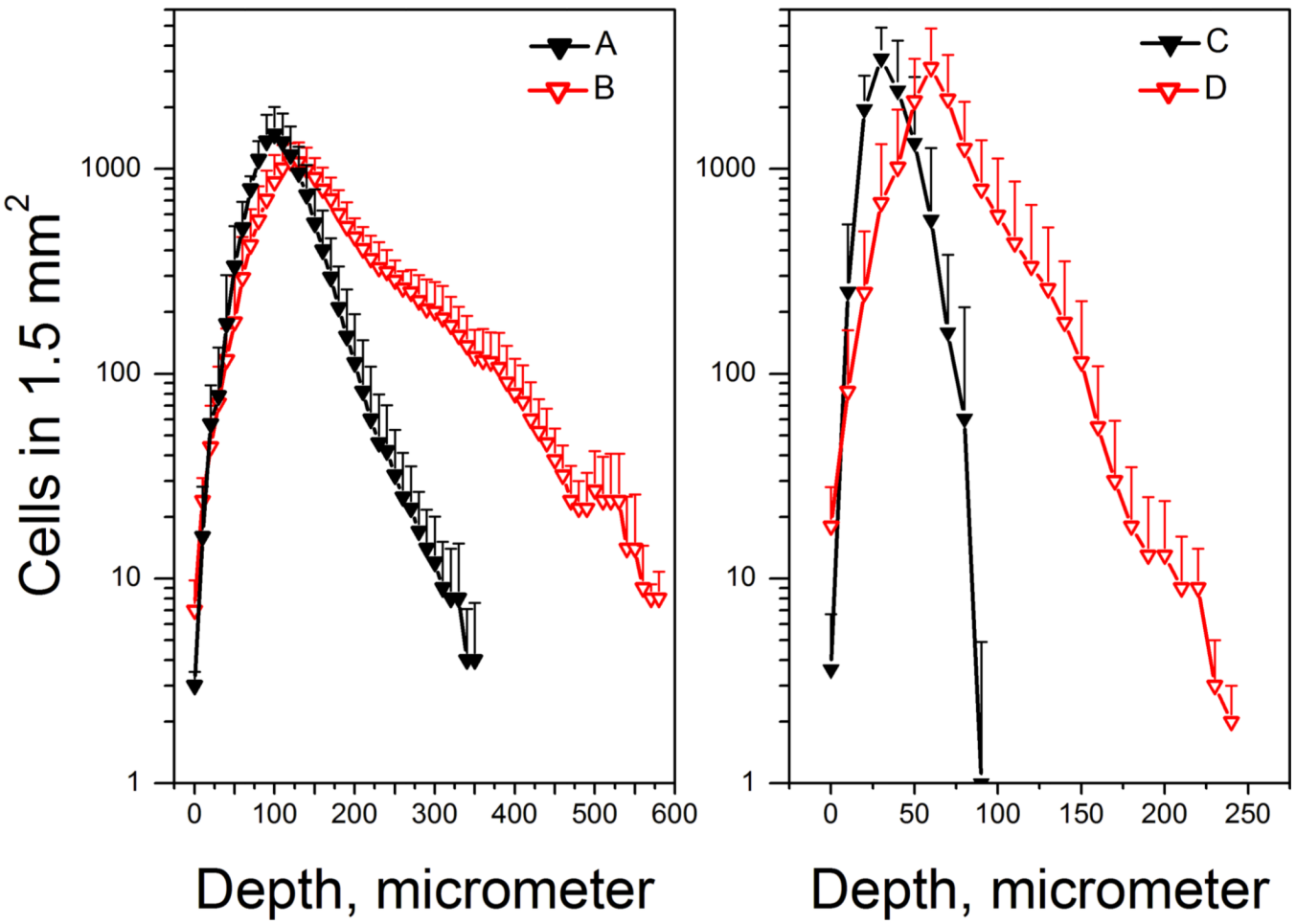


**Figure 8.**
Cellular infiltration into scaffolds. Cell counts as a function of depth into the scaffold are presented: A) FDC, B) PU, C) GNF, and D) TGNF. The bars on graphs represent positive part of the standard deviation.

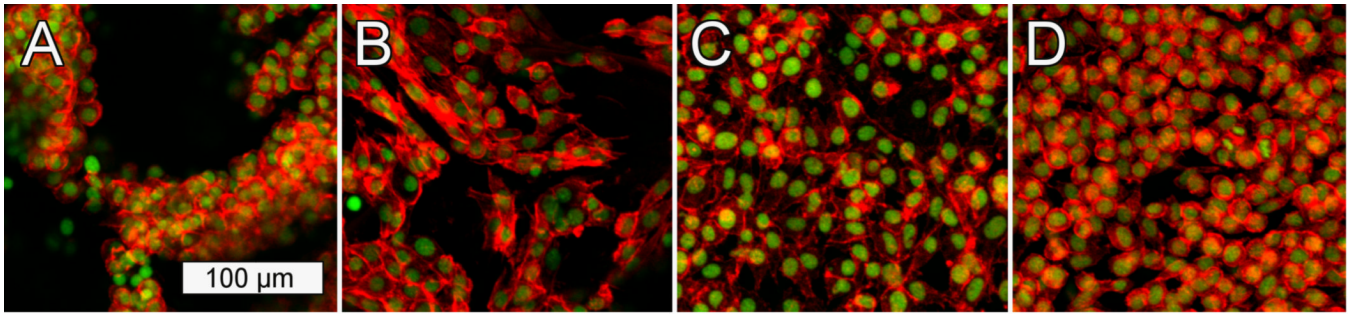


**Figure 9.**
Cytoskeleton and nucleus staining. All images were collected at 20× magnification: A) PU, B) FDC, C) GNF, and D) TGNF. Scale bar is the same for all images.